Simulation of Ridge Formation in Cortical Bone near the Anterior Cruciate Ligament Insertion: Bone Remodeling due to Interstitial Fluid Flow

Yusuke TAKAHASHI, Shigehiro HASHIMOTO

**Biomedical Engineering Laboratory, Department of Mechanical Engineering,
Kogakuin University, Tokyo, 163-8677, Japan
shashimoto@cc.kogakuin.ac.jp http://www.mech.kogakuin.ac.jp/labs/bio/**

and

Hiromichi FUJIE

**Biomechanics Laboratory, Faculty of System Design,
Tokyo Metropolitan University, Tokyo, 191-0065, Japan
fujie@sd.tmu.ac.jp http://www.comp.sd.tmu.ac.jp/fujielab/**

ABSTRACT

The ridge formation in the cortical bone near the anterior cruciate ligament (ACL) insertion has been simulated based on bone remodeling due to interstitial fluid flow. Three-dimensional (3-D) data of cortical bone at the distal end of the femur were obtained from a computer topography image of a human knee joint, and were transformed to a 3-D voxel model consisting of voxel elements of 500 × 500 × 500 μm in size. A finite element analysis software (ABAQUS) was utilized to determine the interstitial fluid flow in the cortical bone in response to the application of ACL tensile force, tibial compressive force, and patellar compressive force. Bone remodeling analysis was repeated until equilibrium in which a new voxel element was added on a surface where local flow rate was higher than predefined thresholds. Results revealed that ridge formation occurred in response to the force application and the ridge structure was dependent on the thresholds of interstitial fluid flow rate.

Keywords: Biomedical Engineering, Finite Element Analysis, Bone Remodeling, Resident's Ridge Formation Anterior Cruciate Ligament and Interstitial fluid flow.

1. INTRODUCTION

Resident's ridge near the anterior cruciate ligament (ACL) on the femoral condyle in the knee joint is clinically used as a landmark to find the bone tunnel position at the surgical ACL reconstruction surgery. Numerous numbers of anatomical researches have been reported as regard with the dimension and structure of the ridge [2-6]. However, the analytical model of femur used in the studies was two dimensions, so it was difficult to simulate to physiological condition. Therefore, we developed a three dimension femoral cortical bone model to perform a precise bone remodeling analysis in the present study. To biomechanically explain the Resident's ridge formation, we hypothesized that due to interstitial fluid flow in response to external loads. The analysis was reported with a variety of the threshold of flow rate. However, the mechanism of formation of the ridge has not been well explained. A 3-D model of the distal femur has been created with the cortical bone in the present study. Meanwhile, the structure of trabecular bone has been biomechanically based on bone remodeling due to compressive strass/strain [7] and interstitial fluid flow [8, 9]. Therefore, Fujie et al proposed that the Resident's ridge formation can be explained by bone remodeling due to compressive strain [10] and interstitial fluid flow [11].

2. METHODS

Finite Elements Model

The cancellous bone of femur, the tibia and patella were removed from the CT image of the human knee joint with the image editing software of GIMP (GNU Image Manipulation Program) (Fig. 1). Finite element model was configured with voxel elements using VOXELCON (QUINT, 2013). The side of voxel was 500 μm. ABAQUS (6.13) was used for finite element analysis in which each element was assumed to be homogeneous and isotropic with elastic modulus of 20 GPa [10] and Poisson's ratio of 0.3. The permeability of the element was 5.13×10^{9} m^2 [12] for the interstitial fluid of 0.001 Pas of viscosity. The pore pressure elements (C3D8RP) were used to visualize the interstitial fluid flow.

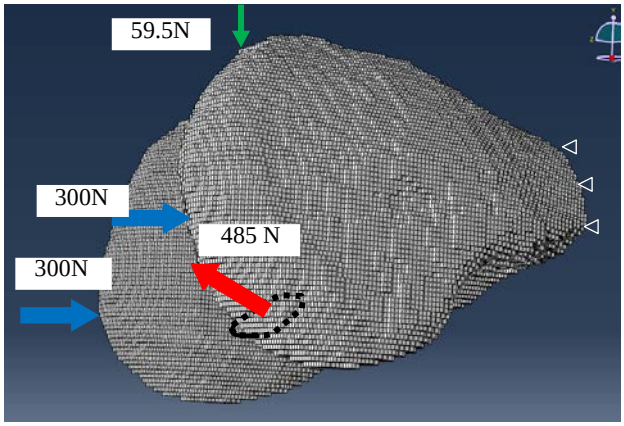

Fig. 1: Three dimensional model of cortical bone at the distal end of femur and forces applied to femur three external.

Calculation

The force applied from the patella to the femur (F_3) was calculated with the following equations,

$$F_1 = F_2 \cos\theta_1 + F_3 \sin\theta_2 \quad (1)$$

$$F_2 \sin\theta_1 = F_3 \cos\theta_2 \quad (2)$$

where F_1 is quadriceps force, while F_2 is the force of patellar ligament force, θ_1 is acute angle between F_1 and F_2, and θ_2 is the complementary angle between F_1 and F_3.

In the present simulation, F1 was set at 136 N, referred from quadriceps using muscles analysis of quadriceps during gate using Opensim. The direction of F_1 was parallel with the bone axis of the femur. θ_1 is 0.43 rad that corresponds to the angle between the bone axis and the patellar ligament. θ_2 was 0.17 rad that corresponds to the flexion angle of the knee joint at the heel strike position in gate.

The point of application of F_3 was referred from the previous anatomical study by Tecklenburg et al. [13]. The position of attachment of the ACL was determined with the previous anatomical study by Andrew et al. [16] and Iriuchishima et al. [17]. The proximal end of femur was fixed while, the force of 300 N was applied on head medical and lateral of the distal end of the femur (Fig. 1).

F_1 was increased to 600 N while F_3 was also increased to the target value for 1s. Subsequently, F_2 was increased to the target value, while F_1 and F_3 were kept constant (Fig.4).

Bone Remodeling Process

The bone remodeling process was started, when F_2 reached to the target value. A new voxel element was added on the element, in which the flow rate exceeds the threshold value of either 0.75, 1.00, 1.25 or 1.50 μm/s, under an assumption that bone formation occurred where local flow rate exceeded the threshold. This calculation process was repeated twice. Note that ACL attachments were elevated to the surface of a remodeled bone voxel (Fig.2).

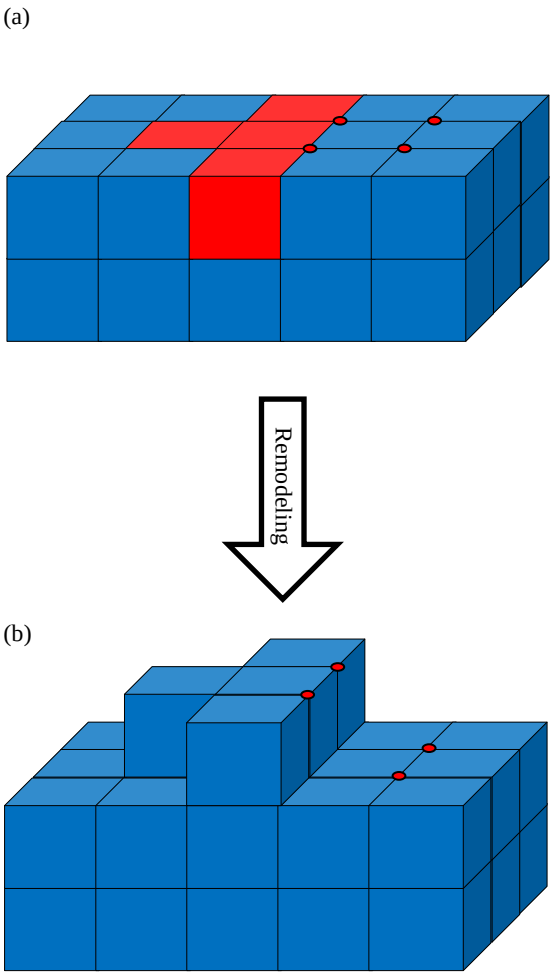

Fig. 2: Upward movement of the ACL insertion to adding elements where the flow rate exceeds thresholds value.

3. RESULTS

Fig. 3 shows the distribution of the flow rate before remodeling calculation started. The direction of interstitial flow rate was almost perpendicular to the surface of the cortical bone (Fig. 4). The high flow rate occurred in the anterior distal area of attachment of the ligament. Figs. 5-8 show the first and second steps of remodeling with the threshold of the flow rate of 0.75 μm/s, 1.00 μm/s, 1.25 μm/s and 1.50 μm/s, respectively.

The area of bone formation decreased as the increase of the threshold of flow rate. Resident's ridge-like bone formation occurred at the thresholds of the flow rate of 0.75 μm/s and of 1.00 μm/s (Figs. 9(A) and 9(B)). On the other hand, such formation did not occurred at the threshold of the flow rate of 1.25 μm/s.

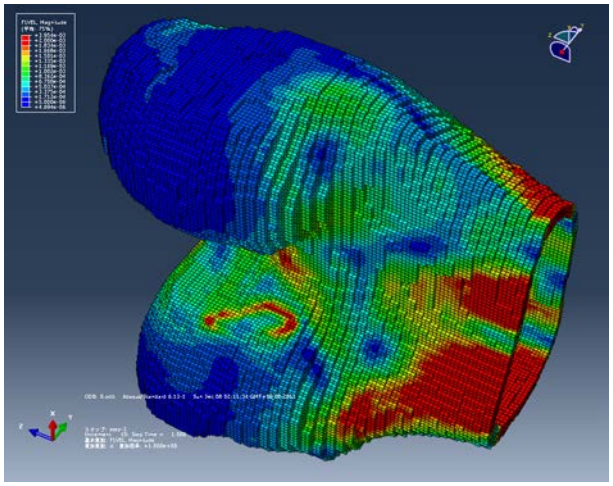

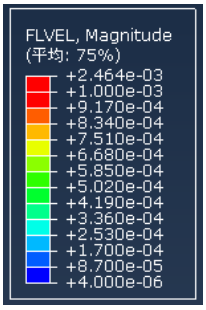

Fig. 3: Distribution of flow rate before the start of remodeling calculation.

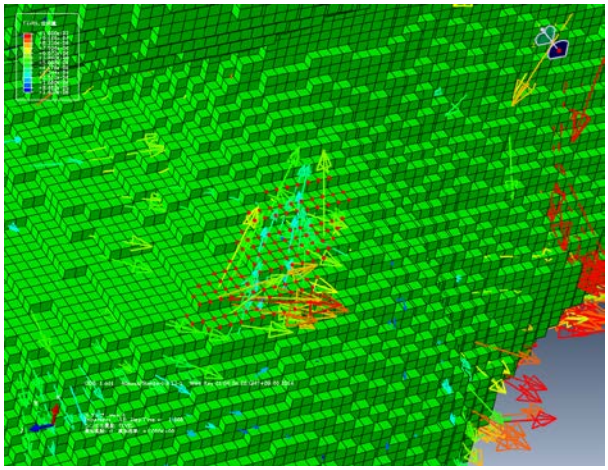

Fig. 4(A): Interstitial fluid flow before the start remodeling calculation at cortical bone surface.

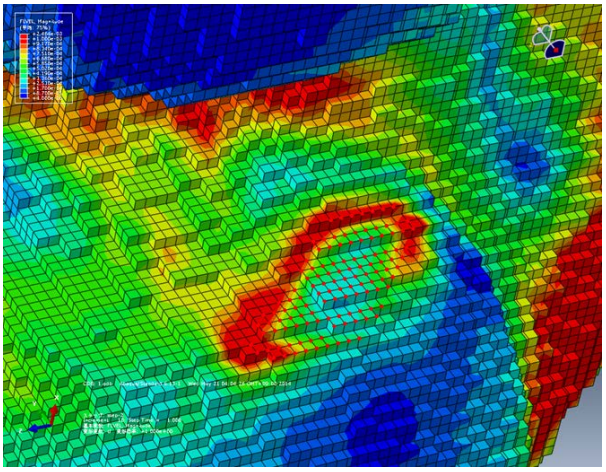

Fig. 4(B): Flow rate distribution at the first step of remodeling calculation

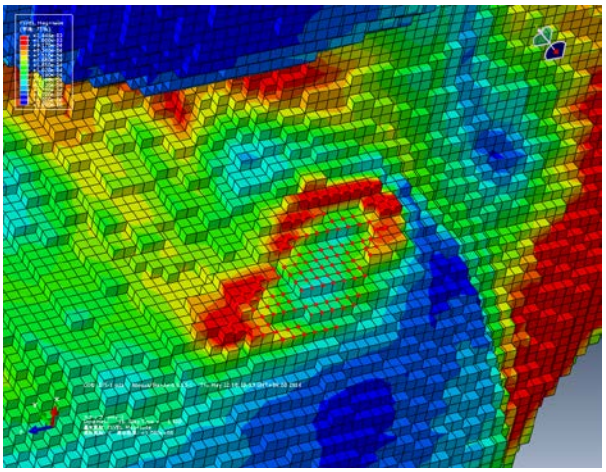

Fig. 5(A): Interstitial fluid flow-induced bone remodeling at the first step of remodeling calculation with a threshold of flow rate of 0.75 μm/s.

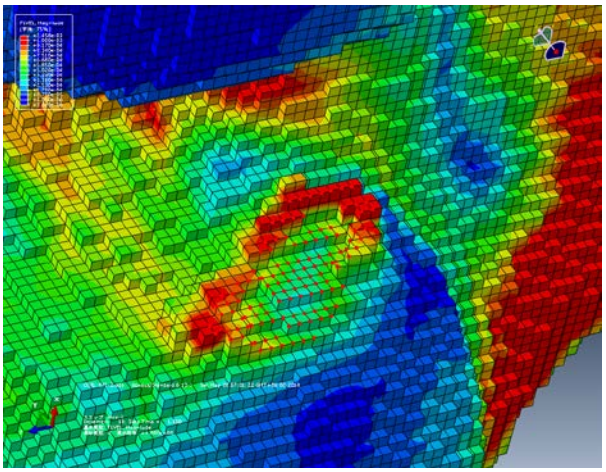

Fig. 5(B): Interstitial fluid flow-induced bone remodeling at the second step of remodeling calculation with a threshold of flow rate of 0.75 μm/s.

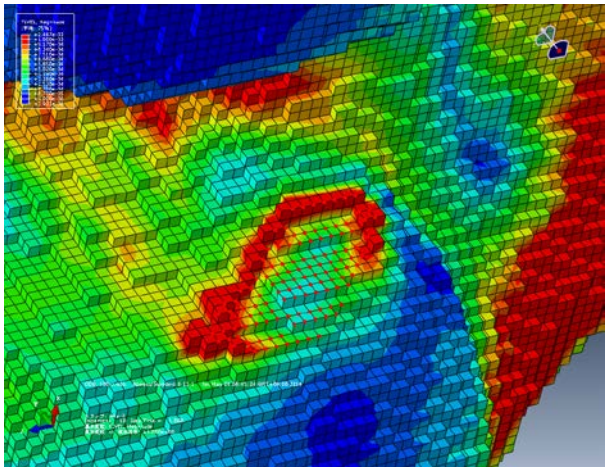

Fig. 6(A): Interstitial fluid flow-induced bone remodeling at the first step of remodeling calculation with a threshold of flow rate of 1.00 μm/s.

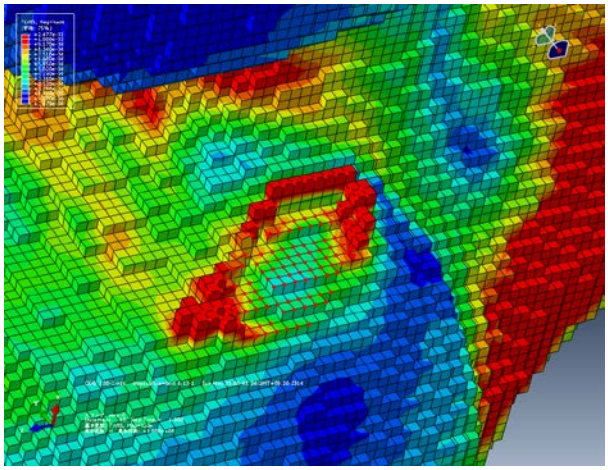

Fig. 6(B): Interstitial fluid flow-induced bone remodeling at the second step of remodeling calculation with a threshold of flow rate of 1.00 μm/s.

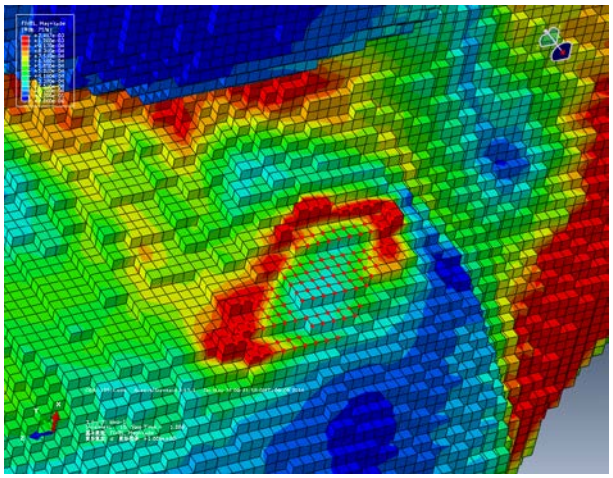

Fig. 7(A): Interstitial fluid flow-induced bone at the first step of remodeling calculation with a threshold of flow rate of 1.25 μm/s.

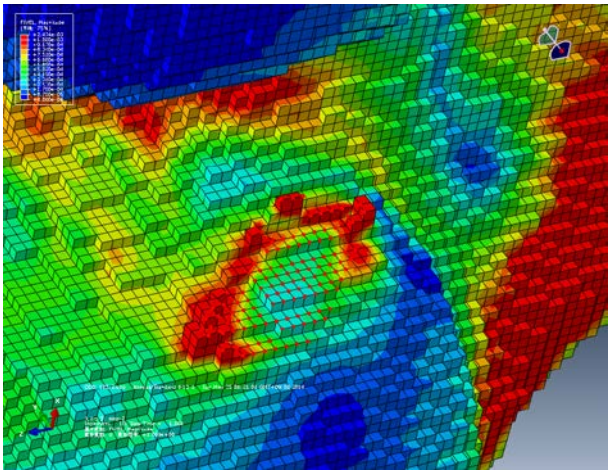

Fig. 7(B): Interstitial fluid flow-induced bone remodeling at the second step of remodeling calculation with a threshold of flow rate of 1.25 μm/s.

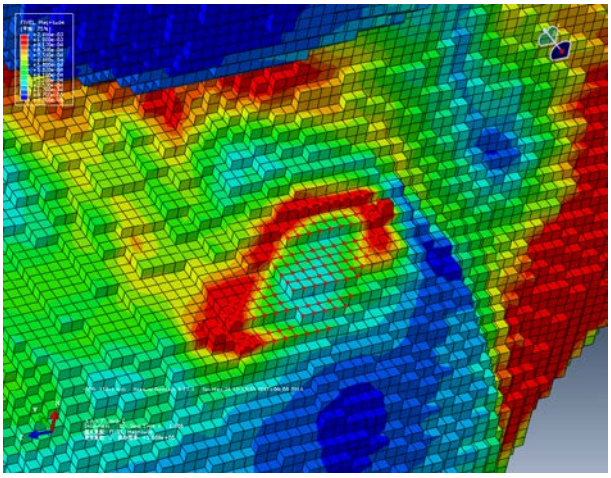

Fig. 8(A): Interstitial fluid flow-induced bone remodeling at the first step of remodeling calculation with a threshold of flow rate of 1.50 μm/s.

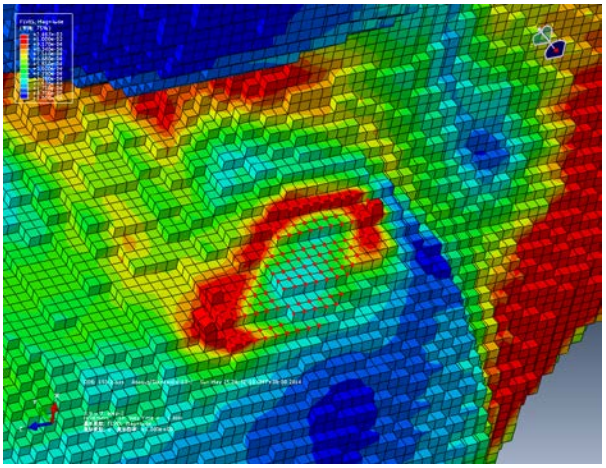

Fig. 8(B): Interstitial fluid flow-induced bone remodeling at the second step of remodeling calculation with a threshold of flow rate of 1.50 μm/s.

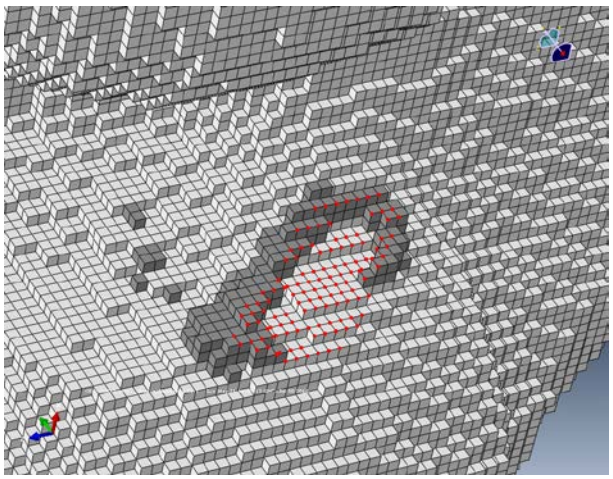

Fig. 9(A): Remodeled bone with a threshold of flow rate of 0.75 μm/s.

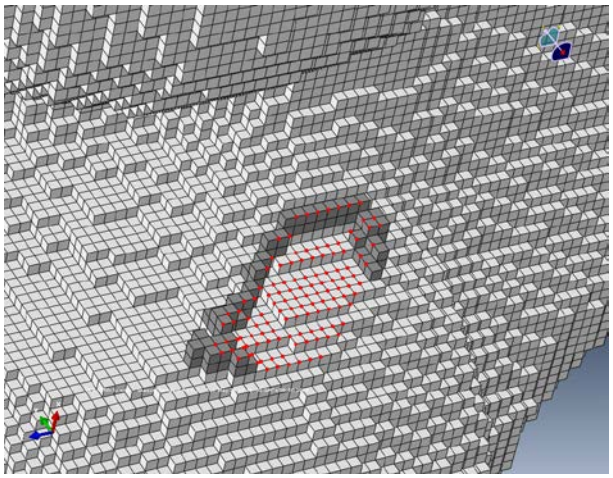

Fig. 9(B): Bone remodeling with a threshold of flow rate of 1.00 μm/s.

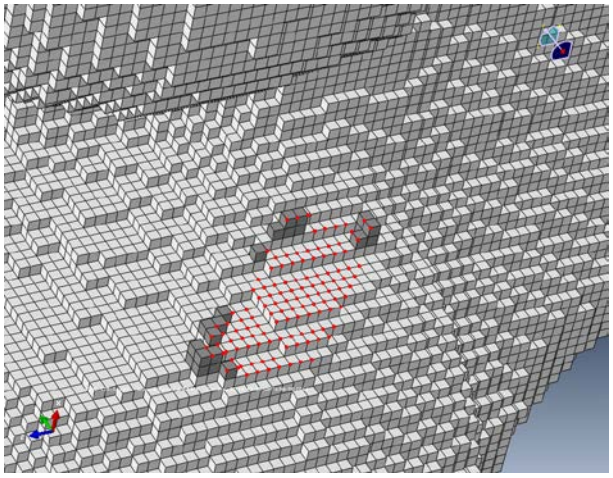

Fig. 9(C): Bone remodeling with a threshold of flow rate of 1.25 μm/s.

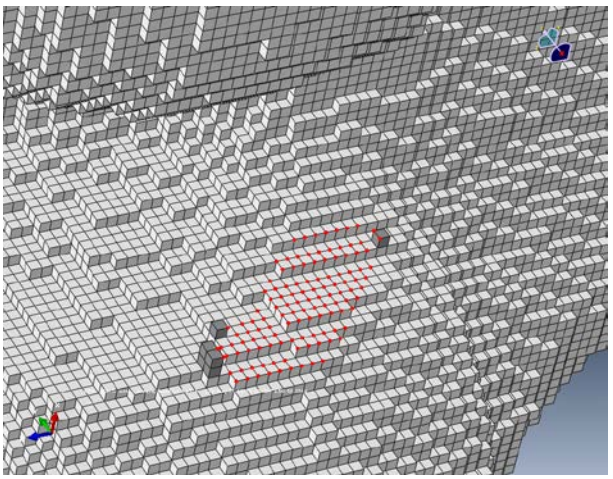

Fig. 9(D): Bone remodeling with a threshold of flow rate of 1.50 μm/s.

4. DISCUSSION

In the present study, the cortical bone remodeling analysis was performed around the ACL insertion site of the femur based on a hypothesis that bone remodeling was caused by interstitial fluid flow. The interstitial fluid flow rate was analyzed in response to three external forces to femur, tibial compressive force, patella compressive force and ACL tensile force. For the analysis, the magnitude and direction of the forces and mechanical properties of the femur were referred from previous literatures. As a result, we succeeded to complete the 3-D analysis as regard with the interstitial fluid rate in the distal femur.

Results revealed that Resident's ridge-liked bone formation occurred at the threshold of relatively low flow rates (0.75 μm/s and 1.00 μm/s) while it did not occur at the threshold of relatively high flow rate (1.25 μm/s and 1.50 μm/s). Weinbaum et al. indicated that osteoblast is stimulated for bone formation when the fluid flow-induced shear stress to the cell exceeds 1 Pa [19]. Although detailed analysis has not been performed, flow-induced shear stress may be adequate for bone remodeling at the flow rate between 0.75 μm/s and 1.00 μm/s.

It is well known that many ridges can be observed near ligament and tendon insertions, such as the tibial tuberosity near tibial insertion of the patella tendon. Further studies possibly explain the mechanism of the formation of three ridges.

5. CONCLUSION

We developed a detailed 3-D model of the distal femur and performed a bone remodeling analysis due to interstitial fluid flow for the explanation of the formation of the Resident's ridge. It was suggested that the Resident's ridge-like bone formation occur at relatively low thresholds of flow rate.

6. ACKNOWLEDGMENT

The present study was supported in part by the Grant-In-Aid for scientific Research B (#25282134) from the MEXT, Japan, the Priority Research Found from Tokyo Metropolitan University,

and the MEXT-Supported Program for the Strategic Research Foundation at Private Universities, 2008-2012 (BERC, Kogakuin University) and 2013-2017 (FMS, Kogakuin University).

REFERENCES

[1] T. Mae, K. Shino, N. Matsumoto, M. Hamada, M. Yoneda and K. Nakata, "Anatomical Two-bundle Versus Rosenberg's Isometric Bi-socket ACL Reconstruction: A Biomechanical Comparison in Laxity Match Pretension", **Knee Surgery, Sports Traumatology, Arthroscopy**, Vol. 15, No. 4, 2007, pp. 328-334.

[2] K. Shino, T. Suzuki, T. Iwahashi, T. Mae, N. Nakamura, K. Nakata and S. Nakagawa, "The Resident's Ridge as an Arthroscopic Landmark for Anatomical Femoral Tunnel Drilling in ACL Reconstruction", **Knee Surgery, Sports Traumatology, Arthroscopy**, Vol. 18, No. 9, 2010, pp. 1164-1168.

[3] F.H. Fu and S.S. Jordan, "The Lateral Intercondylar Ridge - A Key to Anatomic Anterior Cruciate Ligament Reconstruction", **Journal of Bone and Joint Surgery - Series A**, Vol. 89, No. 10, 2007, pp. 2103-2104.

[4] C.F. Van Eck, K.R. Morse, B.P. Lesniak, E.J. Kropf, M.J. Tranovich, C.N. van Dijk and F.H. Fu, "Does the Lateral Intercondylar Ridge Disappear in ACL Deficient Patients?", **Knee Surgery Sports Traumatology Arthroscopy**, Vol. 18, No. 9, 2010, pp 1184-1188.

[5] M.L. Purnell, A.I. Larson and W. Clancy, "Relationships to Critical Bony Landmarks Using High-resolution Volume-rendering Computed Tomography", **American Journal of Sports Medicine**, Vol. 36, 2008, pp. 2083-2090.

[6] Jr.O.V. Lopes, M. Ferretti, W. Shen, M. Ekdahl, P. Smolinski and F.H. Fu, "Topography of the Femoral Attachment of the Posterior Cruciate Ligament", **Journal of Bone and Joint Surgery - Series A**, Vol. 90, No. 2, 2008, pp. 249-255.

[7] R. Ruimerman, P. Hilbers, B. van Rietbergen, R. Huiskes, "A Theoretical Framework for Strain-related Trabecular Bone Maintenance and Adaptation", **Journal of Biomechanics**, Vol. 38, No. 4, 2005, pp. 931-941.

[8] K. Tsubota, T. Adachi and Y. Tomita, "Functional Adaptation of Cancellous Bone in Human Proximal Femur Predicted by Trabecular Surface Remodeling Simulation Toward Uniform Stress State", **Journal of Biomechanics**, Vol. 35, No. 12, 2002, pp. 1541-1551.

[9] T. Adachi, Y. Kameo and M. Hojo, "Trabecular Bone Remodeling Simulation Considering Osteocytic Response to Fluid-Induced Shear Stress", **Philosophical Transactions of the Royal Society A: Mathematical, Physical and Engineering Sciences**, Vol. 368, No. 1920, 2010, pp. 2669-2682.

[10] H. Fujie, S. Yamakawa, K. Nakata and K. Shino, "Resident's Ridge Formation Due to ACL Force-Induced Bone Remodeling" **Proceedings of the Orthopaedic Research Society**: 2013, p. 1383.

[11] Y. Takahashi, S. Hashimoto and H. Fujie, "Finite Element Analysis of Bone Remodeling: Resident's Ridge Formation in Femoral Condyle", **Proc. 17th World Multi-Conference on Systemics Cybernetics and Informatics**, Vol. 1, 2013, pp. 31-33

[12] E.A. Nauman, K.E. Fong and T.M. Keaveny, "Dependence of Intertrabecular Permeability on Flow Direction and Anatomic Site", **Annals Biomedical Engineering**, Vol. 27, No. 4, 1999, pp. 517-524.

[13] A. Edwards, A.M.J. Bull and A.A. Amis, "The Attachments of the Anteromedial and Posterolateral Fibre Bundles of the Anterior Cruciate Ligament: Part 2: Femoral Attachment", **Knee Surgery Sports Traumatology Arthroscopy**, Vol. 16, No. 1, 2008, pp. 29-36.

[14] E.H. Chen and J. Black, "Materials Design Analysis of the Prosthetic Anterior Cruciate Ligament", **Journal of Biomedical Materials Research**, Vol. 14, No. 5, 1980, pp. 567-586.

[15] H. Fujie, H. Otsubo, S. Fukano, T. Suzuki, D. Suzuki, T. Mae and K. Shino, "Mechanical Functions of the Three Bundles Consisting of the Human Anterior Cruciate Ligament" **Knee Surgery Sports Traumatology Arthroscopy**, Vol. 19, No. 1, 2011, pp. 47-53.

[16] T. Iriuchishima, K. Shirakura, H. Yorifuji, S. Aizawa, T. Murakami and F.H. Fu, "ACL Footprint Size is Correlated with the Height and Area of the Lateral Wall of Femoral Intercondylar Notch", **Knee Surgery Sports Traumatology Arthroscopy** , Vol. 21, No. 4, 2013, pp. 789-796.

[17] K. Tecklenburg, D. Dejour, C. Hoser, C. Fink, "Bony and Cartilaginous Anatomy of the Patellofemoral Joint", **Knee Surgery Sports Traumatology Arthroscopy,** Vol. 14, No. 3, 2006, pp. 235-240.

[18] J.C. Lotz, T.N. Gerhart and W.C. Hayes, "Mechanical Properties of Metaphyseal Bone in the Proximal Femur", **Journal of Biomechanical Engineering**, Vol. 113, No. 4, 1991, pp. 317-329.

[19] Weinbaum S., Cowin S.C. and Zeng Y. "A Model for the Excitation of Osteocytes by Mechanical Loading-induced Bone Fluid Shear Stresses", **Journal of Biomechanics**, Vol. 27, No. 3, 1994, pp. 339-360.